Letters

Optically Isolated Rogowski Coil: Non-Invasive Current Measurement With High d*v*/d*t* Immunity for WBG Device

Jiakun Gong, Yulei Wang, Yuxi Liang, Mingrui Zou, Liang Wang, Peng Sun, and Zheng Zeng, *Member, IEEE*

***Abstract*—Rogowski coil (RC) has been extensively employed for current measurement of power devices owning to its non- invasiveness, flexibility and accuracy. However, the increasing blocking voltage and accelerated switching speed of wide-bandgap devices impose significant challenges on RC-based measurement systems, primarily manifested as more severe electric field interference. In this letter, a novel optically isolated Rogowski coil (Opt-RC) is proposed to address the electric field interference issues. By incorporating optical isolation, the original common-mode (CM) interference pathways are effectively interrupted, substantially mitigating CM noise without modifying the coil structure and compromising bandwidth. Furthermore, the excellent insulating properties provided by optical fiber imparts the Opt-RC with significant potential for accurate current measurement in high-voltage scenarios. Comprehensive experiments confirm the electric field interference immunity and excellent insulation of the proposed Opt-RC.**

***Index Terms*—Common-mode (CM) immunity, current sensor, optically isolated Rogowski coil (Opt-RC), wide-bandgap (WBG) device.**

I. Introduction

THE ongoing development of wide-bandgap (WBG) semiconductors, such as silicon carbide (SiC) and gallium nitride, has enabled power devices to achieve higher breakdown voltages and faster switching speeds, thereby enhancing the efficiency and power density of power converters [1]. However, the superior switching performance is accompanied by extremely short switching time and ultrahigh *dv/dt* exceeding 100 V/ns [2], posing significant challenges for accurately capturing their dynamic current. This necessitates current sensors with both high bandwidth and high immunity to electric field interference. In addition, maintaining low invasiveness is critical to avoid perturbing the circuit under test (CUT) that is sensitive to parasitic effects. Among various current measurement solutions, the Rogowski coil (RC) is widely applied in dynamic current measurement of the power devices due to its advantages in galvanic isolation and flexibility [3]. Nevertheless, although the RCs provide inherent electrical isolation, common-mode (CM) currents arising during switching transients can couple into the measurement system through parasitic capacitance pathways, resulting in significant waveform distortion [4].

Some studies have highlighted the CM immunity of the RCs, through strategies such as embedded shielding or winding optimization. In case of embedded shielding, a low-impedance path for the CM currents is provided, effectively protecting the signal winding from electric field interference [5]. In terms of winding optimization, two windings with opposite directions are arranged to form a differential coil, and the CM voltage induced in the same direction on both windings can be efficiently suppressed by the subsequent differential circuit [6]. Previous research has proposed beneficial methods to enhance the CM immunity of RCs for WBG applications. However, both methods require modifications to the original coil structure. The introduction of shielding layers increases the equivalent parallel capacitance within the coil, thereby significantly reducing its bandwidth. Moreover, the addition of shielding may even exacerbate the total CM currents [7]. On the other hand, the differential coils require the two opposing windings to maintain a high degree of structural symmetry, which significantly increases the difficulty of coil design [8]. Additionally, capacitive coupling between the two windings further degrades the bandwidth [9].

To address the aforementioned challenges, a novel optically isolated Rogowski coil (Opt-RC) is proposed. By incorporating optical isolation into the signal chain, the original CM current path is blocked by optical fiber, significantly reducing the interference of CM noise on the measurement system without modifying the coil structure and compromising bandwidth. Furthermore, due to the excellent insulating properties of optical fiber, the proposed Opt-RC holds potential for current measurement in high-voltage environments.

The rest of this letter is organized as follows. In Section II, the basic operating principles and CM-dominated electric field

Received 7 May 2025; revised 1 June 2025; accepted 12 June 2025. Date of publication 16 June 2025; date of current version 5 August 2025. This work was supported in part by the National Natural Science Foundation of China under Grant 52177169, in part by the Chongqing Research Program of Basic Research and Frontier Technology under Grant CSTB2024NSCQ-JQX0016, and in part by the Graduate Research and Innovation Foundation of Chongqing under Grant CYB240023. *(Corresponding author: Zheng Zeng.)*

The authors are with the State Key Laboratory of Power Transmission Equipment Technology, School of Electrical Engineering, Chongqing University, Chongqing 400044, China (e-mail: gonjiakun@cqu.edu.cn; yulei_wang@cqu.edu.cn; yuxiliang@cqu.edu.cn; zoumingrui@cqu.edu.cn; wangliangedu@cqu.edu.cn; sunpeng_96@cqu.edu.cn; zengerzheng@cqu.edu.cn).

Color versions of one or more figures in this article are available at https://doi.org/10.1109/TPEL.2025.3580061.

Digital Object Identifier 10.1109/TPEL.2025.3580061

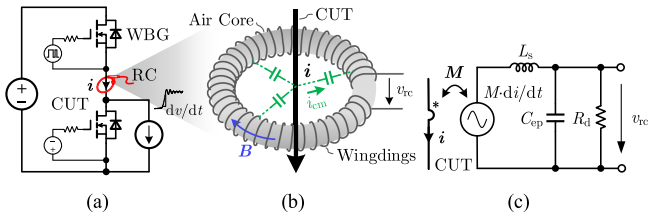

Fig. 1. Operating principle of Rogowski coil. (a) Circuit under test with coil. (b) Physical structure of coil. (c) Equivalent circuit model of coil.

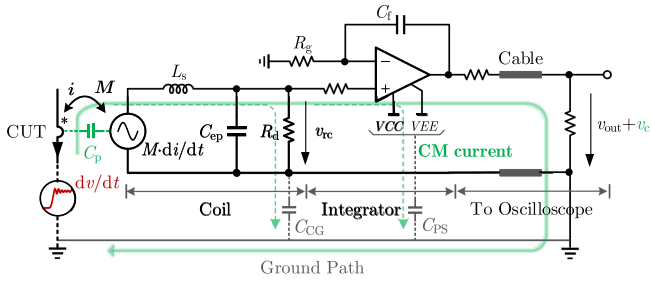

Fig. 2. Illustration of CM current coupling in RC measurement system.

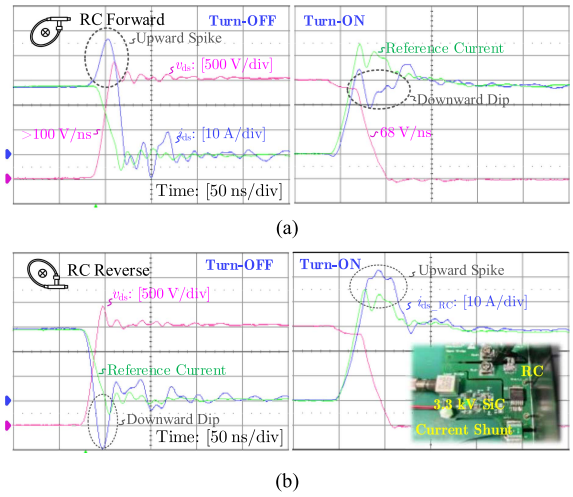

Fig. 3. Impact of electric field interference on commercial RC. (a) RC in forward connection. (b) RC in reverse connection.

interference issues of the traditional RCs are illustrated. In Section III, the principles of the proposed Opt-RC are presented, along with its design methodology. In Section IV, comprehensive experiments in the frequency and time domains are provided to demonstrate the feasibility and effectiveness of the proposed Opt-RC. Finally, Section V concludes this letter.

II. Principle and Electric Field Interference Issues of Traditional Rogowski Coil

A. Operating Principle and Structural Configuration of RCs

The operation principle of the RCs is fundamentally based on Faraday's law of electromagnetic induction. As illustrated in Fig. 1(b), the time-varying current i flowing through the CUT generates an alternating magnetic field, which in turn induces an electromotive force v_s in the coil windings. The relationship between the induced voltage v_s and measured current i is expressed as

$$v_s = -sMi \tag{1}$$

where $s = j2\pi f$ denotes the complex frequency, and M is the mutual inductance between the CUT and the coil.

The equivalent circuit model of the coil, shown in Fig. 1(c), incorporates intrinsic parasitic elements, including the self-inductance L_s and equivalent parallel capacitance C_{ep}. The resulting output voltage v_{rc} across the damping resistor R_d is given by

$$v_{rc} = \frac{-sMR_d \cdot i}{s^2 L_s C_{ep} R_d + sL_s + R_d}. \tag{2}$$

Since the coil's out voltage v_{rc} is proportional to the current derivative, subsequent integration circuits are required to reconstruct the original current waveform. Typically, the bandwidth of commercial RCs is limited to tens of MHz due to the inherent parasitic elements of the coil.

B. Electric Field Interference Issues in RCs

In contrast to the iron-core current transformers, RCs, utilizing an air-core structure, inherently avoid magnetic saturation. Nevertheless, the low magnetic permeability of air imposes a fundamental limitation on the flux linkage, thereby increasing the coil's susceptibility to external electric field interference. The electric field interference issues are exacerbated when the RC is applied in the emerging WBG converter systems where ultra-fast switching speed and miniaturization coexist.

Rapid voltage transients between the CUT and the RC induce non-negligible CM currents, which are coupled into the coil windings and the signal processing circuitry via the capacitive path, as depicted in Fig. 2. These interference currents overlap with the differential-mode measurement signal, leading to substantial distortion in the RC output. When the RC is used to measure the current of high-side devices or drain current of low-side devices, it is directly exposed to severe electric field interference. Moreover, in a compact system layout, even when the RC is used to measure the source current of low-side devices, external electric field interference can still affect the coil through the capacitive coupling path.

The current waveform of 3.3 kV SiC MOSFET operating under high dv/dt conditions is captured using a commercial RC CP9006S, positioned at mid-point of the half bridge to measure the drain current i_d of the lower switch, and the waveform is displayed in Fig. 3. Reference current is obtained by a current shunt with calibrated bandwidth exceeding 3 GHz [10], which is placed at the source of the lower switch and immune to the electric field interference.

It is found that significant distortion of the current waveform appears during the switching transient with high *dv/dt*. However, irrespective of whether the RC is connected in the forward or reverse orientation, the injection direction of high-frequency CM current into the coil remains unchanged, while the measured current polarity is reversed. As a result, during the turn-ON or

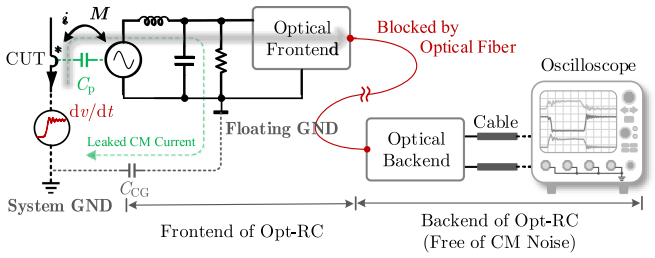

Fig. 4. Mechanism of CM noise suppression in proposed Opt-RC system.

turn-OFF transitions, the associated waveform distortions exhibit opposite polarities for the two configurations, indicating that the distortions are caused by the CM current. Moreover, the increased blocking voltage of the WBG devices demand thicker external insulation layers for coils, while the miniaturization of power semiconductor packages imposes stricter size constraints.

The increased blocking voltage and accelerated switching speeds of WBG devices present significant challenges for the application of RCs, primarily manifested as intensified electric field interference and an elevated risk of insulation breakdown.

III. Principle and Implementation of Proposed Optically Isolated Rogowski Coil

A. Operating Principle of Proposed Opt-RC

To enhance the electric field immunity of RCs, previous studies primarily focused on optimizing coil structures. However, such modifications typically cause a reduction in bandwidth. An alternative and effective approach is to improve the coupling path by incorporating additional isolation or other CM noise reduction circuits. Owning to the high bandwidth and CM interference rejection capability, optical isolation is introduced into the RC's signal path in this letter, offering a novel method to improve CM immunity of the RC-based measurement systems.

In the conventional RC configuration, the reference potentials of the RC system and the power system are typically directly connected via the earth ground or via an isolation transformer, while the capacitive coupling of the isolation transformer presents a low impedance path at high frequency. The internal signal in the RC system typically ranges several volts, while the voltage variations of the device in power system reach hundreds or even thousands of volts with extremely high *dv/dt*. CM currents are induced and flow through parasitic capacitive paths into the coil and subsequent integrator circuit, then propagate via coaxial cable to the oscilloscope before ultimately returning to the earth ground. In particular, the coil-to-ground capacitance C_{CG} and the op-amp's supply-ground coupling capacitance C_{PS} serve as additional paths for high-frequency CM currents to return to the earth ground, as illustrated in Fig. 2.

In contrast, the implementation of optical isolation after the coil enables robust earth decoupling through fiber-optic transmission instead of direct grounding connections, as shown in Fig. 4. The optical frontend operates in a floating state with power supplied by a battery or laser source. The CM currents induced by switching transients are effectively blocked from propagating through the RC's internal circuitry to the optical backend and returning via earth paths. Consequently, the total CM current generated between the CUT and the coil is significantly attenuated, leaking instead through the parasitic capacitance C_{CG} between the coil and the ground. Furthermore, the superior isolation characteristics of optical fibers effectively protect subsequent processing circuits and oscilloscope from CM currents, thereby endowing the Opt-RC with exceptional noise immunity in high electric field environments.

In addition, due to the excellent isolation properties of optical fiber, the Opt-RC maintain high insulating properties without thick external insulation layers. This makes it well-suited for high-voltage, space constrained scenarios, such as current measurement within the high power density converter systems or miniaturized power semiconductor packages by using a coil with small size.

B. Implementation of Proposed Opt-RC

The proposed Opt-RC primarily consists of a coil, an integrator circuit, an optical isolation circuit, and an amplifier to adjust the overall gain, as detailed displayed in Fig. 5. For the coil design, a PCB-based coil featuring fixed geometric parameters and high sensing capability, is designed for both the traditional RC and proposed Opt-RC.

In the integration stage, a combination of passive and active integration is employed to achieve broadband integration characteristics. Specifically, the passive *RC* network is directly connected to the coil output, enabling high-frequency integration while simultaneously attenuating the high-frequency voltage components induced at the coil output, thereby avoiding overdrive of the amplifier. In contrast, the active integrator, provides the required high integration gain at low frequencies.

The optical isolation circuit comprises an optical transmitter that converts the electrical signal to optical signals, and an optical receiver that restores it to an electrical signal, as shown in Fig. 5. The detailed design methodology of the optical isolation circuit is elaborated in [4]. However, applying the optical isolation to the RC, which inherently involves both differentiation, integration and other active circuit, requires additional design considerations. Due to the multi-stage architecture of the RC, the insertion position of the optical isolation circuit significantly impacts the overall performance of the Opt-RC. Three possible insertion positions are shown in Fig. 6.

Position ①: Placed at the output of the coil. The integrator circuit is located on the optical backend, keeping away from interference sources. However, due to the absence of passive integration to attenuate high-frequency components, the sharp current spikes during WBG device switching transients may cause the coil output voltage to exceed the operating range of the optical transmitter circuit.

Position ②: Placed at the output of passive integrator. Due to the coil's weak sensitivity at low-frequency, the signal amplitude is further attenuated after passing through the optical transmitter, making it susceptible to noise. Besides, the dc and low-frequency gain of the active integrator can exceed 80 dB, meaning that even signals as small as tens of μV can be amplified to several

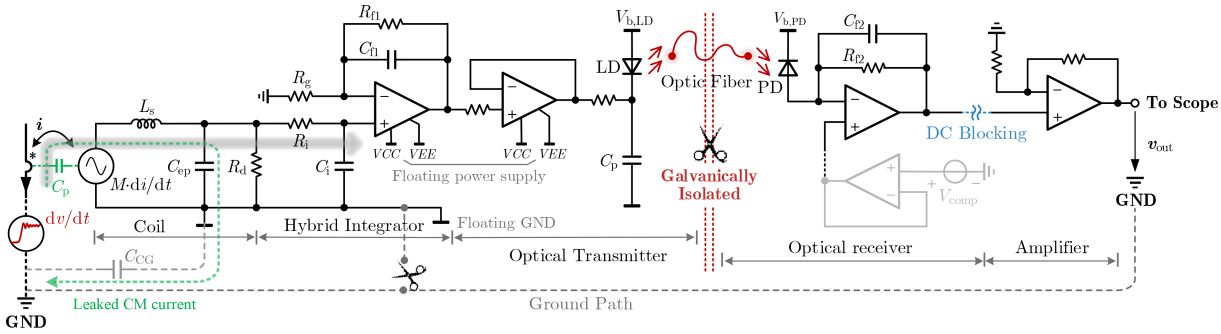

Fig. 5. Circuit schematic of proposed Opt-RC.

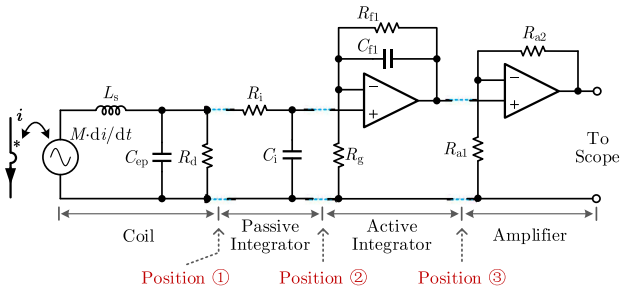

Fig. 6. Insertion positions of optical isolation circuit in RC system.

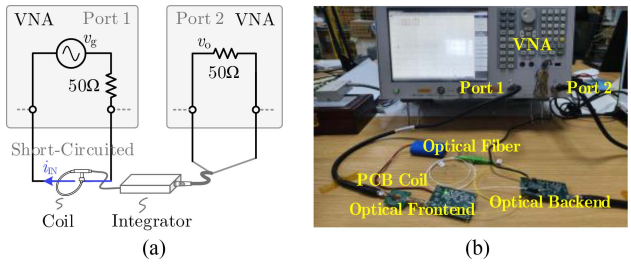

Fig. 7. Calibration principle of RC. (a) Equivalent circuit model. (b) Test rig.

hundred mV. The low-frequency noise coupled in the optical isolation stage is also significantly amplified by several orders of magnitude in the subsequent active integrator. Although this configuration effectively protects the active circuit from CM currents, it may result in substantial low-frequency noise at the output.

Position ③: Placed at the output of active integrator. The coil output, after hybrid integration, maintains a constant gain across the entire operating frequency range and exhibits a high signal-to-noise ratio. Although placing the active integrator at optical frontend may expose it to CM current interference, position ③ is selected in this design to ensure overall performance of Opt-RC, as the active integrator is sensitive to low-frequency noise. In addition, it is recommended to place the optical front-end circuit at a sufficient distance from the noise source via a coaxial cable to minimize the susceptibility of the circuit's small signal to external radiated interference.

Note that, due to the introduction of dc bias and temperature-induced drift by the laser diode in the optical transmitter circuit, compensation for both dc offset and the thermal drift is required in optically isolated voltage probe systems. In contrast, since the RC is an ac current sensor with no dc component in the valid signal, the dc drift can be simply removed by inserting a dc-blocking stage after the trans-impedance amplifier, as shown in Fig. 5. Moreover, the trans-impedance gain is carefully constrained to prevent op-amp saturation caused by amplified dc bias. And an amplifier circuit is placed after the dc-blocking circuit to compensate the overall gain.

It is critical that the optical isolation circuit does not compromise the bandwidth of the original RC system. To this end, a unit-gain amplifier TI LMH6559 with bandwidth of 1.75 GHz is used in the optical transmitter circuit. LD and PD with 2.5 GHz analog bandwidth are employed to construct the optical signal path. The TI OPA818 is used to build the high-bandwidth trans-impedance amplifier circuit, with a gain-bandwidth product of 2.7 GHz and a high operating voltage of ±5 V. For even higher optical isolation bandwidth, the TI OPA855 can be used as the trans-impedance amplifier, though its operating range is limited to ±2.5 V. The detailed circuit parameter design can be referred to [4]. Currently, the bandwidth of commercial RCs does not exceed 100 MHz. Therefore, the OPA818 is sufficient to meet the bandwidth requirements. Optical components with lower bandwidth can be used to further reduce the cost.

IV. Experimental Validations and Analyses

A. Bandwidth Calibration of Proposed Opt-RC

A vector network analyzer (VNA) E5061B is used to evaluate the frequency-domain characteristics of the designed Opt-RC. The calibration principle and test setup are displayed in Fig. 7. The port 1 of the VNA is short-circuited to convert the voltage signal into current signal, which then passes through the center of the coil under test. The RC output is connected to port 2 of the VNA, enabling precise calibration of the RC.

Both the traditional RC and proposed Opt-RC exhibit a bandwidth of approximately 60 MHz, as shown in Fig. 8. The calibration results indicate that the introduction of optical isolation does not compromise bandwidth of original measurement system. Besides, the high-bandwidth capability of optical isolation enables its potential application in RC measurement systems requiring broader bandwidths. In terms of signal-to-noise ratio,

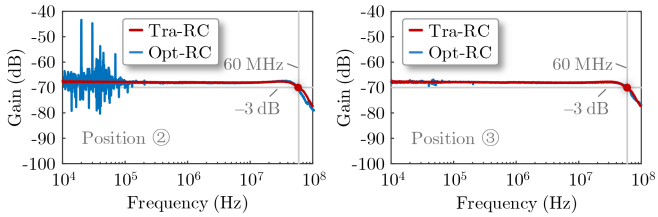

Fig. 8. Frequency characteristics (10 kHz-100 MHz) of traditional RC and proposed Opt-RC. (a) Optical isolation at position ②. (b) Optical isolation at position ③.

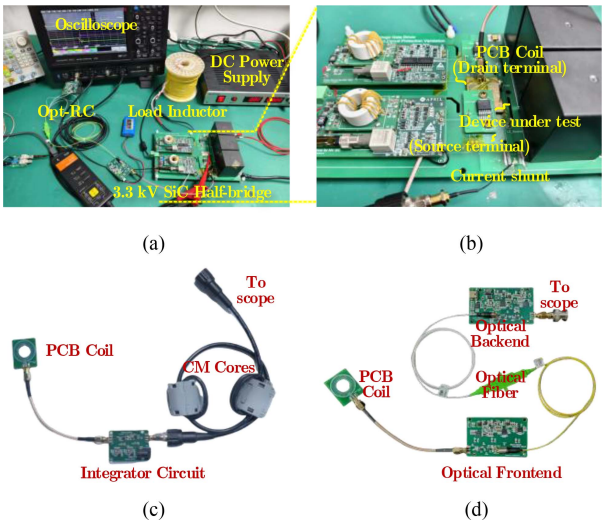

Fig. 9. *Dv/Dt* immunity verfication based on 3.3 kV double-pulse test rig. (a) Double pulse test rig. (b) Positions of the coil and current shunt in the half-bridge circuit. (c) Prototype of Tra-RC with CM cores. (d) Prototype of proposed Opt-RC.

when inserted at position ③, the low frequency noise caused by the optical isolation circuit is significantly reduced compared to position ②.

B. Electric Field Interference Immunity Verification Based on 3.3 kV Double-Pulse Test Platform

To evaluate the electric field interference immunity of the proposed Opt-RC, a double-pulse test platform is constructed using the 3.3 kV SiC MOSFET with extra-high *dv/dt,* as shown in Fig. 9(a). In addition, the high bandwidth current shunt is placed at the source terminal of the lower switch to obtain the reference current, and the PCB coil is alternately installed at either the drain or source terminals of the lower switch, to evaluate the RC's performance under varying external electric interference conditions, as displayed in Fig. 9(b). The device current is measured using three distinct RC configurations: the traditional RC (Tra-RC); the traditional RC with CM cores added to the output coaxial cable (Tra-RC+CM Cores), as shown in Fig. 9(c); and the proposed Opt-RC, as displayed in Fig. 9(d).

The experimental results are displayed in Fig. 10. When the coil is placed at the mid-point of the half-bridge, where *dv/dt* exceeds 100 V/ns, the output of traditional RC exhibits

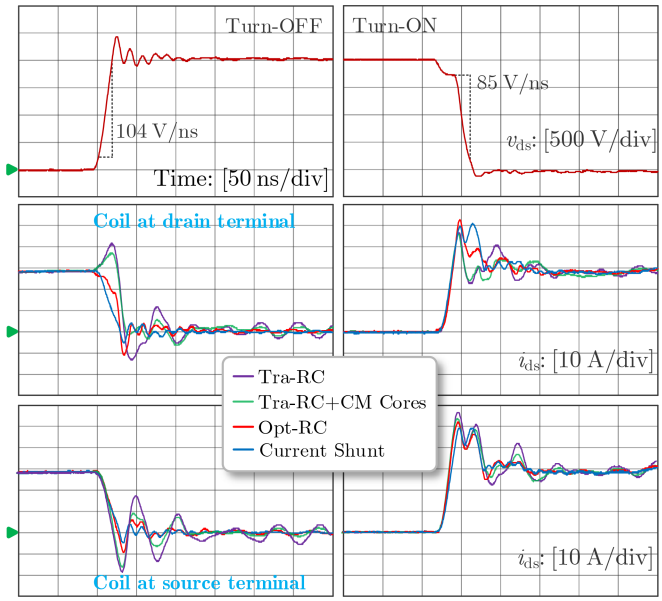

Fig. 10. Measured switching trajectories by using Tra-RC, Tra-RC+CM Cores, and proposed Opt-RC.

severe distortion. Moreover, the flow of CM currents within the RC measurement system introduces significant waveform oscillations. Even when positioned at the source terminal of the lower switch, the coil remains susceptible to external field interference due to the compact layout of the test setup. Note that the reversed current direction at the source alters the effect of the external field on the coil's output. Building on the traditional *RC* setup, the coaxial cable connected to the oscilloscope is wound around two ferrite cores (ZCAT3035-1330, TDK) to suppress CM noise on the path without degrading signal integrity. Experimental results show that the addition of CM cores effectively attenuates post-switching oscillations in the current waveform. However, its effectiveness in mitigating distortions caused by high *dv/dt* transients remained limited. In contrast, the Opt-RC exhibits significantly enhanced immunity to the interference. Oscillations induced by CM current are effectively suppressed, and the measured switching transients closely align with those obtained using the current shunt.

However, some discrepancies remain between the measurements of the Opt-RC and those of the current shunt. The first factor is the lower measurement bandwidth of the RC. The second factor is the coil's direct exposure to extremely high *dv/dt* exceeding 100 V/ns, where optimizing the CM current path alone is insufficient to fully eliminate the induced electric field interference. Optimization of the coil can be further combined to realize more accurate current measurement under the extremely harsh electric field conditions.

C. Insulation Performance Verification Based on 10 kV Double-Pulse Test Platform

In addition to enhancing electric field immunity, the optical isolation substantially improves the coil's insulation performance without the need for thick external insulation layers. The

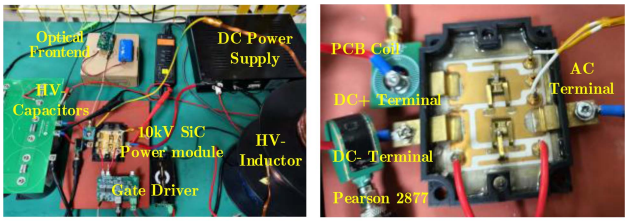

(a) (b)

Fig. 11. High-voltage double-pulse test platform based on 10 kV SiC half-bridge power module. (a) Double-pulse platform. (b) Positions of the coil and Pearson 2877 on the 10 kV half-bridge power module.

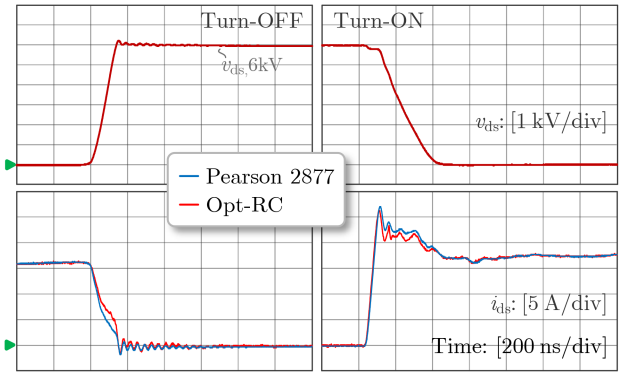

Fig. 12. Current waveform measured by Pearson 2877 and proposed Opt-RC under 6 kV DC-Link voltage.

insulation capability of the proposed Opt-RC is validated using a high-voltage double-pulse test platform based on a custom-packaged 10 kV SiC half-bridge power module, as illustrated in Fig. 11(a). The 10 kV, 15 A SiC MOSFET chips are provided by CETC, and subsequently processed with Ni/Pd/Au surface metallization by Chuangzhi Semi-link Technology Co.,Ltd.

The PCB coil is mounted on the dc+ terminal of the power module for high-voltage current measurements, with only a thin solder mask layer as external insulation. For reference measurements, a current transformer Pearson 2877 with bandwidth of 200 MHz is placed in the source-to-capacitor return path of the lower switch, as shown in Fig. 11(b).

Experimental results demonstrate that the optically isolated system reliably measured device currents at a 6 kV bus voltage, achieving comparable accuracy to the Pearson 2877, as shown in Fig. 12. The superior insulation capability of the optical fiber maintains the coil in a fully floating state, while the optical back-end, oscilloscope, and operator remain at a safe low potential. While the PCB coil is employed for parameter control, the optical isolation method can be further applied to flexible coils with small size, enabling flexible and nonintrusive current measurement in high-voltage, high-*dv/dt* and space constrained scenarios, such as current measurement in high power density converters or miniaturized power module packaging.

V. Conclusion

In this letter, the Opt-RC with enhanced electric field immunity is proposed for non-intrusive current measurement of WBG devices. By introducing high bandwidth optical isolation, the original CM current path is interrupted, thus significantly reducing the electric field interference experienced by the RC, without compromising the bandwidth of the original measurement system. Considering the inherent characteristics of the RC measurement system, the implementation of the proposed Opt-RC is discussed to achieve low noise and high bandwidth. Comparative experiments validate the effectiveness of the proposed Opt-RC in enhancing electric immunity for emerging WBG applications. Besides, the insulation performance of the Opt-RC is validated using the 10 kV SiC double-pulse test platform. The optical isolation technology can be further applied to the flexible coils with small size, making it well-suited for high-voltage, high-*dv/dt*, and space constrained scenarios. Although the optical isolation approach presents higher cost and system complexity compared to conventional solutions, its superior *dv/dt* immunity and enhanced insulation performance establish the Opt-RC as a promising current measurement solution for harsh electric environments.

References

[1] D. Rothmund, T. Guillod, D. Bortis, and J. W. Kolar, "99% efficient 10 kV SiC-based 7 kV/400 V DC transformer for future data centers," *IEEE J. Emerg. Sel. Top. Power Electron.*, vol. 7, no. 2, pp. 753–767, Jun. 2019.

[2] C. DiMarino et al., "Design and experimental validation of a wire-bondless 10-kV SiC MOSFET power module," *IEEE J. Emerg. Sel. Top. Power Electron.*, vol. 8, no. 1, pp. 381–394, Mar. 2020.

[3] H. Li, Z. Gao, R. Chen, and F. Wang, "Improved double pulse test for accurate dynamic characterization of medium voltage SiC devices," *IEEE Trans. Power Electron.*, vol. 38, no. 2, pp. 1779–1790, Feb. 2023.

[4] Y. Wang et al., "Flexible 1.5-GHz probe isolation extension with high CMRR and Robust d*v*/d*t* immunity empowering next-generation WBG measurement," *IEEE Trans. Power Electron.*, vol. 40, no. 1, pp. 862–878, Jan. 2025.

[5] J. Wang, Z. Shen, R. Burgos, and D. Boroyevich, "Integrated switch current sensor for short circuit protection and current control of 1.7-kV SiC MOSFET modules," in *Proc. IEEE Energy Convers. Congr. Expo.*, 2016, pp. 1–7.

[6] J. N. Fritz, C. Neeb, and R. W. Doncker, "A PCB integrated differential Rogowski coil for non-intrusive current measurement featuring high bandwidth and d*v*/d*t* immunity," in *Proc. Power Energy Student Summit*, 2015, Paper S05.2.

[7] X. Zhao et al., "Design of ultracompact gate driver integrated with current sensor and commutation path for a 211-kW three-level SiC aircraft propulsion inverter," *IEEE J. Emerg. Sel. Top. Power Electron.*, vol. 11, no. 4, pp. 4077–4094, Aug. 2023.

[8] C. Hewson and J. Aberdeen, "An improved Rogowski coil configuration for a high speed, compact current sensor with high immunity to voltage transients," in *Proc. IEEE Appl. Power Electron. Conf. Expo.*, 2018, pp. 571–578.

[9] Y. Shi, Z. Xin, P. C. Loh, and F. Blaabjerg, "A review of traditional helical to recent miniaturized printed circuit board Rogowski coils for power-electronic applications," *IEEE Trans. Power Electron.*, vol. 35, no. 11, pp. 12207–12222, Nov. 2020.

[10] Y. Wang et al., "Miniaturized current shunt with high bandwidth and low parasitics for high-integrated applications: Electro-thermal considerations and co-design," *IEEE Trans. Power Electron.*, vol. 39, no. 12, pp. 15732–15747, Dec. 2024.